Intelligent Fusion of Multi-Modal Data in Power Systems and Graph-Driven Collaborative Optimization Method

Qi Chen*, Wei Wang, Yun Dong and Chunfang Yi

Guangxi Power Grid Co. Ltd., Nanning, Guangxi 530000, China
E-mail: QiChen_9801@outlook.com
**Corresponding Author*

Received 08 May 2026; Accepted 23 June 2026

Abstract

As the digital transformation of new power systems accelerates, advanced applications – such as source-grid-load-storage coordination and fault diagnosis – demand real-time perception and intelligent decision-making from multi-modal data. Yet power data is inherently multi-source heterogeneous, spatiotemporally cross-regional, and strongly coupled. Traditional methods suffer from semantic fragmentation and imprecise parsing, making it hard to meet the requirements for high-reliability, adaptive, and low-risk operation and control. This research focuses on the intelligent fusion of multi-modal power data and knowledge graph-driven collaborative optimization, aiming to achieve a closed-loop enhancement from data to decision. The main work includes: (1) constructing a multi-modal power knowledge graph for source-grid-load-storage collaboration scenarios, integrating multi-source information such as equipment, operation, faults, and procedures to form a knowledge base with spatiotemporal attributes and causal relationships; (2) designing semantic parsing and pattern linking algorithms based on graph learning and attention mechanisms to achieve accurate and interpretable mapping from natural language to structured data, and introducing an executability

Journal of ICT Standardization, Vol. 14_4, 507–536.
doi: 10.13052/jicts2245-800X.1441
© 2026 River Publishers

verification and feedback mechanism to improve the robustness and security of queries; (3) developing a graph service and correction module that supports edge-cloud collaboration to provide flexible and reliable data intelligence support for wide-area protection, fault diagnosis, low-carbon scheduling, and other businesses. Experiments show that the proposed method significantly improves the accuracy of cross-modal queries and the robustness of semantic parsing, and verifies its engineering practicality and closed-loop control enhancement capabilities in scenarios such as distribution situation awareness, relay protection risk warning, and energy storage coordination control.

Keywords: Knowledge graph, power data, graph learning, attention mechanism, semantic parsing.

1 Introduction

The new power system exhibits typical characteristics of high proportion of new energy, wide-area distributed interconnection, and deep coordination of source, grid, load, and storage. The operating mechanism has shifted from "source follows load" to "multi-dimensional interaction of source, grid, load, and storage". This transformation places extremely high demands on the real-time perception, cross-temporal, and spatial correlation and intelligent decision-making capabilities of multi-modal operation data. However, power data covers multiple heterogeneous modalities such as time series measurement, equipment status, fault recording, meteorological environment, and regulation text. It has characteristics such as different temporal and spatial scales, heterogeneous physical semantics, and complex coupling relationships. The traditional decision-making paradigm based on a single data source or simple rules is difficult to support the high reliability, adaptive, and low risk operation control requirements [1]. In recent years, knowledge graphs have gained widespread attention in the fields of power equipment management, fault diagnosis, and dispatch assistance due to their unique advantages in the unified representation of heterogeneous data and complex correlation modeling [2].

Liu et al. proposed a knowledge graph construction method for the spatial layout of underground powerhouses in pumped storage power stations, aiming to solve the problems of missing design parameter cascade logic and difficulty in retrieving standard cases. The results showed that the question-answering system developed based on the knowledge graph could effectively

realize knowledge query and parameter recommendation, providing support for the digital intelligent design of underground powerhouses [3]. Yang et al. proposed a design method that integrates meta-knowledge graph and event state knowledge graph, which is used to configure components of physical system and state monitoring system, and to model interaction, operation, and intelligent decision-making mechanisms. The experiment took the robot grinding line as an example. The results showed that the method could not only realize static configuration, but also realize the formal expression and reasoning of dynamic process and intelligent function through the self-updating event state knowledge graph [4]. Sun et al. proposed a temporal neural probabilistic logic learning framework to realize the prediction of future unknown facts, to address the problem that existing methods in temporal knowledge graph reasoning cannot make full use of time information and complex temporal relationship patterns at the same time. The results showed that the framework achieved better performance on multiple benchmark datasets, especially in scenarios where prior knowledge was available but data samples are sparse [5]. Xu et al. proposed a top-down method for constructing a knowledge graph of hydropower station scheduling and operation procedures to address the problems of low structure and lack of knowledge support for fault handling. This method constructs a pattern layer by extracting terms and relations, and uses a bidirectional gated recurrent unit-conditional random field (BiGRU-CRF) model to extract entities to fill the data layer. The results showed that the constructed knowledge graph of hydropower station scheduling and operation could provide auxiliary decision-making for fault handling for staff, and effectively improve the level of emergency management and scheduling intelligence [6].

Although the above research has laid an important foundation for the field of electric power knowledge graph, it can be found through sorting that existing methods still have deep limitations from “data representation” to “semantic understanding” and then to “service architecture". Firstly, in terms of knowledge construction, the work of Liu et al. [3] and Xu et al. [6] focuses on structured or semi-structured data, while the configuration method of Yang et al. [4] considers dynamic processes, but its ability to extract unstructured text and waveforms at a fine-grained level is still limited, making it difficult to cope with the heterogeneous gap of multi-modal data in power systems. Secondly, in terms of semantic parsing, current methods, such as Sun et al.’s [5] temporal inference framework, mainly rely on template matching or sequence annotation, lacking modeling and executable verification of deep level query

intent, resulting in insufficient mapping accuracy and robustness from natural language to structured queries. Finally, in terms of service deployment, the above studies all adopt a centralized architecture, which fails to solve the collaborative contradiction between edge real-time response and cloud global optimization in wide area distributed scenarios. Based on this, this study proposes a collaborative optimization method for intelligent fusion of multi-modal data and graph-driven optimization in power systems, aiming to achieve closed-loop enhancement from multi-modal data to executable decisions and overcome the bottlenecks of semantic fragmentation and insufficient collaborative optimization capabilities of heterogeneous data in power systems. The innovations of this method are: (1) constructing a multi-modal knowledge graph of electricity that integrates spatiotemporal attributes and causal relationships to achieve unified representation and dynamic inference capabilities of cross-source heterogeneous knowledge; (2) proposing a semantic parsing method that combines graph attention mechanism and executability feedback verification to improve the recognition accuracy and robustness of complex query intents; (3) designing an adaptive graph service and bidirectional correction framework for edge-cloud collaboration to achieve dynamic collaboration of knowledge distribution, service scheduling and model evolution.

2 Method and Materials

To achieve closed-loop enhancement from multimodal data to executable decisions, the method design in Section 2 follows a progressive logic of "knowledge base→semantic understanding→collaborative services", with clear driving and supporting relationships between the three. Specifically, the multi-modal knowledge graph of power constructed in Section 2.1 serves as a unified knowledge base, providing structured entity, relationship, and pattern constraints for subsequent semantic parsing. Section 2.2 proposes a graph attention semantic parsing and pattern linking method, which uses this knowledge graph as the query target to achieve precise conversion from natural language to executable query statements, and the results directly serve upper level decision-making applications. The edge cloud collaborative graph service framework designed in Section 2.3 addresses the deployment and evolution of knowledge graphs in widely distributed scenarios based on the first two parts. Through knowledge distribution and bidirectional correction mechanisms, it ensures the real-time and reliability of semantic parsing and decision-making tasks. The three form a complete technological chain of

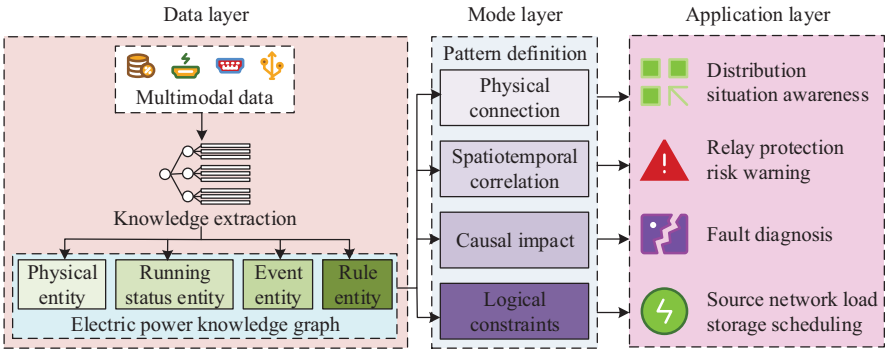


Figure 1 Power multi-modal knowledge graph architecture.

building knowledge with diagrams, illustrating semantics with diagrams, and promoting collaboration with diagrams.

2.1 Knowledge Graph Construction for Multi-Modal Power Data

With the in-depth development of new power systems, various links in the power generation, grid, load, and storage systems generate multi-modal data, including time-series measurements, equipment condition monitoring, environmental meteorology, fault recordings, and regulatory texts. These data exhibit significant heterogeneity and strong coupling characteristics in terms of spatiotemporal scale, physical semantics, and structure, making it difficult for traditional methods based on single data sources or simple rules to achieve cross-spatial collaborative analysis and decision-making. Knowledge graphs, by uniformly representing multi-source heterogeneous entities and their complex relationships, can construct an interpretable domain knowledge base, providing structured support for subsequent intelligent analysis and collaborative optimization. Therefore, constructing a multi-modal power knowledge graph with spatiotemporal and causal reasoning capabilities is a prerequisite for achieving intelligent data fusion, and its architecture is shown in Figure 1.

As shown in Figure 1, the knowledge graph constructed in this study adopts a layered architecture of "data layer – schema layer – application layer". In the data layer, four core entities are defined: physical entities, operational status entities, event entities, and rule entities. Furthermore, to achieve the transformation from multi-modal raw data to structured knowledge, a hybrid knowledge extraction process was designed, as shown in Figure 2.

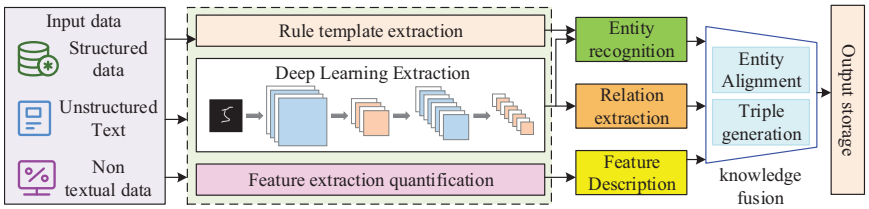


Figure 2 Hybrid knowledge extraction process.

As shown in Figure 2, the hybrid knowledge extraction process adopts differentiated methods for different modal data. For structured and semi-structured data, first map database table fields or XML tags to predefined classes and attributes in the ontology, then convert each record into a triple form of entity relationship attribute according to the mapping rules. For unstructured text, a sequence annotation model is used to identify entity boundaries and types in the text, then a relationship classifier is used to determine the semantic relationships between entity pairs, outputting triplets with confidence scores. For image and waveform data, convolutional neural networks are first used to extract deep features, then the feature vectors are mapped to probability distributions of predefined state categories through fully connected layers. The state descriptor corresponding to the highest probability is taken as the output, and finally the state descriptor is associated with the corresponding physical entity as a node value [7, 8]. At the pattern layer, a system covering four core relationships – physical connection, spatiotemporal correlation, causal influence, and logical constraint – is defined to take into account both the physical characteristics and operational logic of the power system. To characterize dynamic causal chains, a predecessor-successor causal edge based on statistical learning initialization of historical event sequences is introduced [9]. By attaching effective time intervals and spatial coordinates to entities and relationships, spatiotemporal attribute descriptions of the graph are realized, supporting historical retrospection and situational deduction.

In addition, in response to the potential conflicts and ambiguities in entity descriptions in multi-source data, the study adopts a combination of attribute similarity calculation and domain rule verification for entity alignment. The fused knowledge is stored in the graph database in the form of a resource description framework graph and is linked with the original multi-modal data to ensure the traceability of knowledge [10]. The graph pattern is explicitly defined by the Web Ontology Language, providing a unified semantic constraint and reasoning basis for upper-layer applications. The graph quality

is iteratively optimized through consistency verification and expert review, and finally a multi-modal power knowledge graph covering multiple links of source, grid, load, and storage, integrating static parameters, dynamic data, event records, and domain rules is formed. The construction process can be summarized by the following mathematical expression of core relation extraction and alignment. For any two entities e_i and e_j, the establishment of their relationship r_{ij} depends on multi-source evidence E_{ij} and is quantified by confidence c_{ij}, as shown in Equation (1).

$$r_{ij} = \arg\max_{r \in R} \sum_{e \in E_{ij}} \omega_e \cdot \sin(f(e), g(r)) \tag{1}$$

where R is a predefined set of relations, $f(\cdot)$ and $g(\cdot)$ are the feature mapping functions of evidence and relations, respectively, $sim(\cdot)$ is the similarity calculation function, and ω_e is the weight of the corresponding evidence source, which is dynamically adjusted according to the reliability and timeliness of the data source [11]. The entity alignment problem can be formalized as finding the optimal mapping function $\Phi : E' \to E$, so that the aligned entity set satisfies the global consistency constraint to the maximum extent.

2.2 Power Semantic Parsing and Pattern Linking Based on Graph Attention and Feedback Verification

While power multi-modal knowledge graphs can provide structured and semantic representations of underlying data, achieving graph-driven collaborative optimization applications requires accurately mapping the query intent expressed by users or business systems in natural language or semi-structured form to the corresponding entities, relationships, and patterns in the graph. Considering that traditional template-based or statistical learning methods often struggle to accurately capture deep semantic relationships, this study proposes a semantic parsing and pattern linking method that integrates graph attention mechanisms and executability feedback verification. This aims to achieve accurate, robust, and secure conversion from natural language queries to executable graph queries, providing a reliable foundation for intent understanding in subsequent collaborative optimization. The method employs a continuous processing flow of semantic encoding, pattern matching, query graph generation, and feedback verification, as shown in Figure 3.

As shown in Figure 3, the semantic encoding stage converts the query text into a sequence of word vectors through a pre-trained language model in the

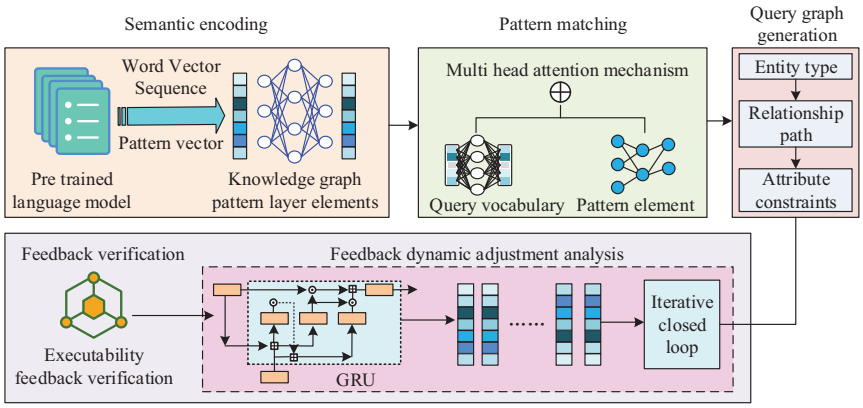


Figure 3 Continuous processing flow.

power field, and maps the knowledge graph pattern layer elements into pattern vectors. The pattern matching stage constructs a bipartite graph structure of query words and pattern elements, uses a multi-head attention mechanism to calculate semantic association weights, and identifies the correspondence between key information fragments in the query and graph patterns [12]. The query graph generation stage constructs a structured query template based on semantic alignment results and syntactic analysis, and clarifies the entity type, relation path, and attribute constraints to be retrieved. To ensure the accuracy and security of queries, research introduces an executable feedback verification mechanism. The specific workflow of this mechanism is first to submit the structured query template output from the query graph generation stage to the graph database execution engine for lightweight probe queries [13]. This probe query does not return a complete result set, but only verifies whether the query syntax is correct, whether the entities and relationships referenced in the query exist in the graph pattern layer, and whether attribute constraints conflict with predefined value ranges. The results returned by the probe query include three types of feedback signals: syntax validity flag, missing element list, and type mismatch alarm. Subsequently, the above three types of feedback signals are encoded into fixed length feedback feature vectors. Finally, the feedback feature vector is concatenated with the query semantic representation and pattern semantic representation of the current round, and input into the gate controlled loop unit. The correction module dynamically adjusts the attention weight allocation and query graph generation strategy in the next round of parsing process, forming an iterative optimization loop of “generation verification correction". Meanwhile, embedding security policy

checks in this closed loop to filter query intentions involving permission violations or sensitive data access. Among them, the graph attention calculation can be expressed as Equation (2).

$$\alpha_{ij}^{(k)} = \frac{\exp(\sigma(\mathbf{a}_k^T[\mathbf{h}_i \| \mathbf{e}_j]))}{\sum_{l=1}^{m} \exp(\sigma(\mathbf{a}_k^T[\mathbf{h}_i \| \mathbf{e}_l]))} \tag{2}$$

where $\mathbf{h}_i$ is the semantic vector representation of the ith query vocabulary, obtained from the output of a pre-trained language model in the field of electricity, $\mathbf{e}_j$ is the embedding vector of the jth pattern element, trained through the names and descriptive texts of pattern layer entities in the graph database, $\|$ represents vector concatenation operation, and the dimension after concatenation is 1024, $\mathbf{a}_k$ is the learnable parameter vector of the kth attention head, with a total of 8 attention heads, σ is the LeakyReLU activation function, with a negative slope coefficient of 0.2. The exponential function $\exp(\cdot)$ is used to map activation values to non-negative weights. m is the total number of pattern elements [14]. $\alpha_{ij}^{(k)}$ is the normalized attention weight between query vocabulary i and pattern element j in the k th attention head, with a value range of [0,1] and satisfying $\sum_{j=1}^{m} \alpha_{ij}^{(k)} = 1$. The optimization objective function for query graph generation can be expressed as Equation (3).

$$\mathcal{L}_{\text{gen}} = \sum_{v \in V_q} \mathbf{A}_{i,\text{type}(v)} + \sum_{e \in E_q} \mathbf{A}_{i,\text{pred}(e)} - \lambda \cdot \text{Complexity}(G_q) \tag{3}$$

where V_q and E_q are the sets of nodes and edges in candidate query graph G_q, respectively. $\mathbf{A}$ is the semantic alignment matrix, and its element $\mathbf{A}_{i,\text{type}(v)}$ represents the alignment score between the ith vocabulary in the query and the entity type of node v. $\mathbf{A}_{i,\text{pred}(e)}$ represents the alignment score between the predicate of the relationship between the ith word in the query and edge e. Both types of alignment scores are obtained by calculating the attention weights using Equation (2) and averaging them through multi head weighting [15]. $\text{Complexity}(G_q)$ is the complexity measurement function of the query graph, specifically defined as $\text{Complexity}(G_q) = |V_q| + |E_q| + \sum_{p \in Path(G_q)} len(p)$, where $|V_q|$ and $|E_q|$ are the number of nodes and edges, respectively. $Paths(G_q)$ is the set of all simple paths in the query graph, and $len(p)$ is the number of edges of path p. This function aims to penalize complex query structures with too many nodes, too many edges, or excessively long inference paths. λ is a hyperparameter that controls the complexity of the query graph, with a value range of [0.01, 0.1]. In this study,

the value is 0.05 . $\mathcal{L}_{\text{gen}}$ is the objective function value generated by the query graph, and the optimization objective is to select G_q from the candidate query graphs that maximizes $\mathcal{L}_{\text{gen}}$. The feedback correction process realizes the iterative update of the semantic representation through the gated loop unit, as shown in Equation (4).

$$[\mathbf{h}'_t; \mathbf{e}'_t] = \text{GRU}([\mathbf{h}_{t-1}; \mathbf{e}_{t-1}], \mathbf{f}_{t-1}) \tag{4}$$

where $\mathbf{h}_{t-1}$ is the semantic representation of the query before the $t-1$th round of correction, $\mathbf{e}_{t-1}$ is the semantic representation of the pattern before the $t-1$th round of correction, and the two are concatenated as the hidden state input of GRU, with a concatenation dimension of 1024. $\mathbf{f}_{t-1}$ is the feedback feature vector obtained in the $t-1$ th round, which is encoded from the three types of feedback signals returned by the probe query and used as the input feature of GRU. $[\mathbf{h}'_t; \mathbf{e}'_t]$ is the semantic representation after the tth round correction, where $\mathbf{h}'_t$ and $\mathbf{e}'_t$ are restored to 768 and 256 dimensions through splitting operations. The GRU unit adopts a single-layer structure with a hidden state dimension of 10241024, which is consistent with the input concatenation dimension. The gate controlled loop unit achieves iterative optimization of the parsing process by updating and resetting the gate to control the degree of correction of semantic representation feedback information. Based on the above, a precise and robust conversion from natural language query to executable graph query can be achieved, thereby effectively supporting intelligent interaction and decision-making based on knowledge graphs in various business scenarios of the power system.

2.3 Support for Edge-Cloud Collaborative Graph Services and Intelligent Correction Framework

While semantic parsing and pattern linking methods can provide accurate query and interaction capabilities for power knowledge graphs, practical applications in widely distributed power systems place higher demands on data real-time performance, service reliability, and decision-making agility. To address the collaborative needs of local data processing at the edge, rapid response, global optimization in the cloud, and knowledge accumulation, a graph service and intelligent correction framework supporting edge-cloud collaboration was designed. This framework aims to achieve distributed deployment of graph services, collaborative evolution of knowledge, and adaptive optimization of models, as shown in Figure 4.

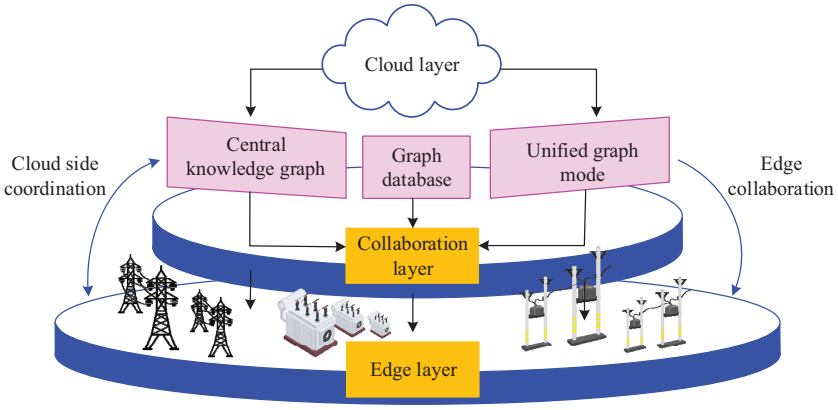


Figure 4 Intelligent correction framework.

Figure 4 shows the intelligent correction framework, which follows the overall principles of cloud-side coordination, edge execution, and bidirectional collaboration, and constructs a three-layer architecture including the edge layer, the collaboration layer, and the cloud layer. In the cloud layer, the central knowledge graph serves as a global knowledge base, storing multimodal structured knowledge after network fusion through a graph database, and maintaining a unified graph pattern, parsing model, and optimization algorithm [16]. The edge layer is deployed in substations, distribution terminals, and distributed energy sites in various regions. Each edge node dynamically loads the corresponding knowledge subgraph from the cloud as a local knowledge cache according to its geographical scope and business responsibilities, and runs a lightweight inference engine to support millisecond-level real-time queries. The collaboration mechanism between the edge and the cloud is shown in Figure 5.

As shown in Figure 5, the collaboration mechanism between the edge and the cloud is achieved through three core processes: knowledge distribution, service collaboration, and two-way correction. Knowledge distribution adopts an adaptive push strategy based on business scenarios. The cloud layer calculates the required knowledge subgraph range based on the functional characteristics of the edge nodes and determines the distribution content through the following optimization objectives, as shown in Equation (5).

$$\min_{S_e} \left(\alpha \cdot \text{Size}(\mathcal{S}_e) + \beta \cdot \sum_{r \in \mathcal{R}_e} \text{Freq}(r) \cdot \text{Dist}(r, \mathcal{S}_e) \right) \tag{5}$$

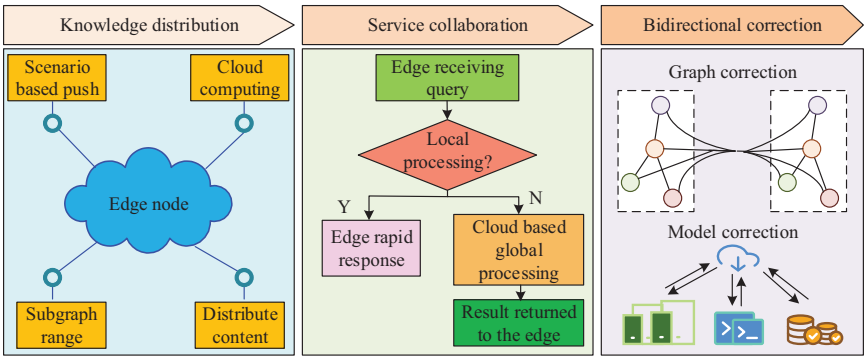


Figure 5 Schematic diagram of the core process of the collaborative mechanism.

where $\mathcal{S}_e$ represents the set of knowledge subgraphs assigned to edge node e. Measure the storage overhead of quantum graph Size$(\cdot)$ and assess the local storage burden of edge nodes. $\mathcal{R}_e$ is a common set of query patterns for edge nodes, which is based on historical query log statistics. Freq(r) is the access frequency of query pattern r, reflecting the popularity of this pattern on edge nodes. Dist$(r, \mathcal{S}_e)$ represents the reachability distance of pattern r in subgraph $\mathcal{S}_e$, defined as the sum of the shortest path lengths involved in the pattern, used to measure the support efficiency of the subgraph for a specific query. α and β are trade-off parameters that respectively control the relative importance of storage overhead and query efficiency in the optimization objective [17]. The optimization objective is to prioritize the distribution of knowledge subgraphs with high frequency and low accessibility distance under limited storage resources, to achieve the optimal balance between edge node query hit rate and response delay.

In the knowledge distribution strategy, business scenario characteristics are quantified through the scenario labels of edge nodes and historical query behavior. Each node is labeled with one or more scene tags based on its deployment location, such as "Distribution Situation Awareness" and "Relay Protection Verification". Cloud maintenance scenario knowledge mapping matrix records the strength of the association between each scenario label and knowledge graph elements, which is obtained based on the access frequency statistics in historical query logs. For nodes, candidate knowledge elements are extracted from the mapping matrix based on their scene labels and assigned initial weights. Then, the weights are dynamically updated using exponential weighted moving average combined with recent query logs. Finally, the optimal knowledge subgraph is solved using Equation (5) as the

objective function, where the query pattern set is composed of high-frequency queries, $\mathrm{Freq}(r)$ is calculated using dynamic weights, and $\mathrm{Dist}(r, \mathcal{S}_e)$ is pre calculated using the shortest path algorithm.

Service collaboration establishes an intelligent task scheduling mechanism. When the edge node receives a query request, it first evaluates the query complexity and the completeness of local knowledge, as shown in Equation (6).

$$\mathrm{Decision}(q) = \begin{cases} \text{LocalProcess}, & \text{if Complexity } (q) \\ & \quad \leq \theta_c \wedge \text{ Coverage } (\mathcal{S}_c, q) \geq \theta_v \\ \text{CloudProcess}, & \text{otherwise} \end{cases} \tag{6}$$

where $\mathrm{Complexity}(q)$ represents the complexity score of the query, Coverage $(\mathcal{S}_c, q)$ measures the coverage of the local knowledge subgraph to the query requirements, θ_c and θ_v are the decision thresholds [18]. Local processing ensures real-time performance, while cloud processing ensures global optimality. The bidirectional correction mechanism includes two dimensions: graph correction and model correction. Graph correction uses data anomalies and knowledge conflicts collected during edge execution as feedback signals, while the cloud layer uses an anomaly detection algorithm based on graph neural networks (GCN) to identify potential errors, as shown in Equation (7).

$$\mathcal{E}_{\text{anomaly}} = \{e \mid \sigma(\mathbf{h}_e) > \gamma, e \in \mathcal{G}\} \tag{7}$$

where $\mathbf{h}_e$ is the embedding representation of the entity $e, \sigma(\cdot)$ is the anomaly scoring function, γ is the anomaly threshold, and $\mathcal{E}_{\text{anomaly}}$ is the set of anomaly entities that need to be corrected [19]. Model correction utilizes edge query logs to optimize the semantic parsing model and employs a federated learning framework for distributed training, as shown in Equation (8).

$$\mathbf{w}_{t+1} \leftarrow \mathbf{w}_t - \eta \cdot \frac{1}{|\mathcal{E}|} \sum_{e \in \mathcal{E}} \nabla F_e(\mathbf{w}_t) \tag{8}$$

In Equation (8), $\mathbf{w}_t$ is the model parameter of the t th round, η is the learning rate, $F_e(\cdot)$ is the local loss function of the edge node e, and ε is the set of nodes participating in the training [20, 21]. Based on the above, the system construction from centralized knowledge management to distributed intelligent services can be completed, realizing the dynamic collaboration, continuous optimization and reliable service of power knowledge at the edge and cloud, and providing unified and elastic architectural support for intelligent decision-making in multiple business scenarios of new power systems.

3 Results

3.1 Performance Verification and Analysis

To verify the effectiveness of the designed method, an experimental evaluation was conducted. The experimental data came from the actual operation dataset of a provincial power grid company in China from 2022 to 2024, covering transmission, substation, distribution, and distributed energy links. This included approximately 15 TB of time-series measurement data, over 80,000 equipment status text reports, 23,000 fault recording files, and related dispatching procedures and standard documents. In terms of data preprocessing, linear interpolation was used to fill in missing values for time-series measurement data, and abnormal jump points were removed based on the 3 σ criterion. Text reports underwent word segmentation, stop word removal, and sentence boundary detection. The fault recording file was resampled at a uniform sampling rate, and effective segments from the first four cycles to the last eight cycles of the fault were captured. The constructed knowledge graph contained a total of 426,000 entities and approximately 1.87 million relationship edges, of which physical connection relationships accounted for 38%, spatiotemporal correlation relationships accounted for 25%, causal influence relationships accounted for 22%, and logical constraint relationships accounted for 15%. The experimental platform consisted of a cloud server cluster and six simulated edge nodes. The cloud configuration included 4 GPU servers, each equipped with 2 NVIDIA Tesla A100 graphics cards and 256 GB of memory. Neo4j graph database and PyTorch model training environment were deployed. The edge nodes adopted embedded industrial control computers, equipped with 8-core ARM processors, 16 GB memory, and 128 GB solid-state drives, simulating on-site computing units. The experimental platform consisted of a cloud server cluster and six simulated edge nodes. The cloud was configured with a high-performance graph database and model training environment, while the edge nodes used embedded industrial control computers to simulate on-site computing units. The experiment first evaluated the construction quality of the multi-modal knowledge graph; the results are shown in Table 1.

Table 1 shows that the entity and relation extraction F1 scores for structured data both exceeded 98.5%, demonstrating the best performance. For unstructured text, the entity and relation extraction F1 scores reached 94.5% and 93.4%, respectively. The feature association F1 score for non-text data was 95.7%. After entity alignment and conflict resolution, the overall knowledge graph consistency F1 score reached 97.2%, indicating

Table 1 Performance evaluation of multi-modal knowledge extraction

Data Modality	Evaluation Metric	Precision (%)	Recall (%)	F1 Score (%)
Structured data	Entity extraction	99.5	98.7	99.1
	Relation extraction	98.9	98.2	98.5
Unstructured text	Entity extraction	95.2	93.8	94.5
	Relation extraction	94.7	92.1	93.4
Non-text data	Feature association	96.4	95	95.7
Overall	Knowledge graph consistency	N/A	N/A	97.2

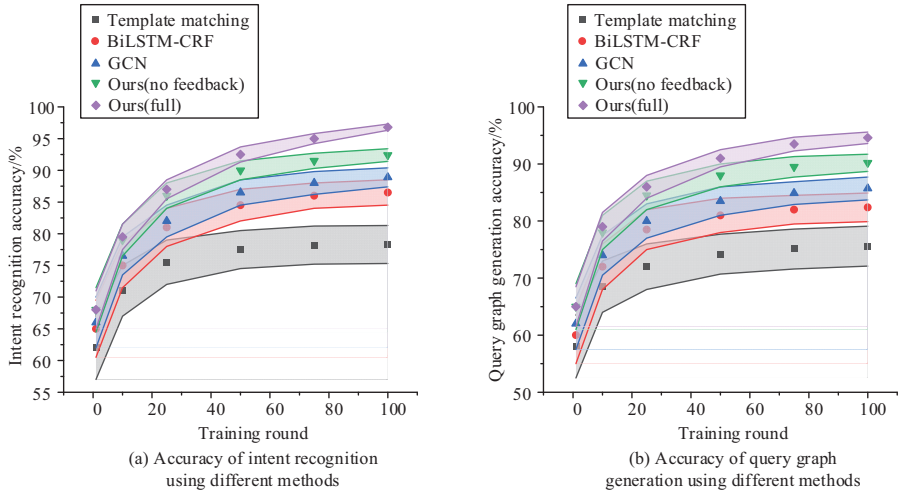


Figure 6 Performance comparison of semantic parsing and pattern linking.

that multi-modal knowledge extraction possessed high accuracy and usability. Next, the semantic parsing and pattern linking method based on graph attention and feedback verification was tested. The experiment selected 500 natural language query statements covering equipment queries, fault tracing, and operation mode adjustments, and compared them with bidirectional long short-term memory-conditional random field (BiLSTM-CRF) model, and classic GCN model. The results are shown in Figure 6.

As shown in Figure 6(a), the intent recognition accuracy of all five methods improved with training rounds. The template matching method plateaued early at 78.3%. BiLSTM-CRF and GCN reached 86.5% and 88.9%, respectively. The two proposed methods started from a higher baseline: the version without feedback achieved 92.4%, while the complete version

Table 2 Semantic parsing performance comparison on difficult samples (%)

Difficult Sample Type	Evaluation Metric	Complete Method	Version Without Feedback
Long-tail query	Intent recognition accuracy	89.7	82.4
	Query graph generation correctness	86.4	78.3
	Intent recognition accuracy	91.2	84.4
	Query graph generation correctness	88.5	81.1

with feedback verification reached the highest accuracy of 96.8% through continuous mid-to-late stage optimization. Figure 6(b) shows query graph generation accuracy. Template matching achieved 75.6%. BiLSTM-CRF and GCN converged to 82.4% and 85.7%, respectively, with GCN benefiting from its structural modeling advantages. Among the proposed methods, the version without feedback reached 90.2%, while the complete version with feedback verification continuously corrected the query graph structure, achieving a leading accuracy of 94.6%.

To further evaluate the robustness of semantic parsing methods on difficult samples, two types of difficult samples, long-tail queries and fuzzy expressions, were selected from 500 test queries, accounting for 12% and 8%, respectively. Among them, long-tail queries refer to query statements involving low-frequency entities or rare relationship paths, whose corresponding knowledge graph pattern elements appear less than five times in the training set. Fuzzy expression refers to queries that involve natural language ambiguity phenomena such as synonym substitution, unclear reference, or omission of key components. The test results of the two methods on difficult samples are shown in Table 2.

According to Table 2, the complete method outperformed the non-feedback version in all metrics on two types of difficult samples, with an 8.1% improvement in query graph generation accuracy for long-tail queries. In contrast, the template matching method had an intention recognition accuracy of less than 65% on both types of difficult samples. The above results validated the robustness advantage of the graph attention mechanism and feedback verification collaborative method for difficult samples.

For the edge-cloud collaborative graph service framework, experiments were conducted to evaluate its service efficiency and resource optimization effects. The experiments simulated high-concurrency query scenarios and compared the performance of three modes: pure cloud processing, static edge caching, and dynamic collaborative distribution as presented in this study. The results are shown in Figure 7.

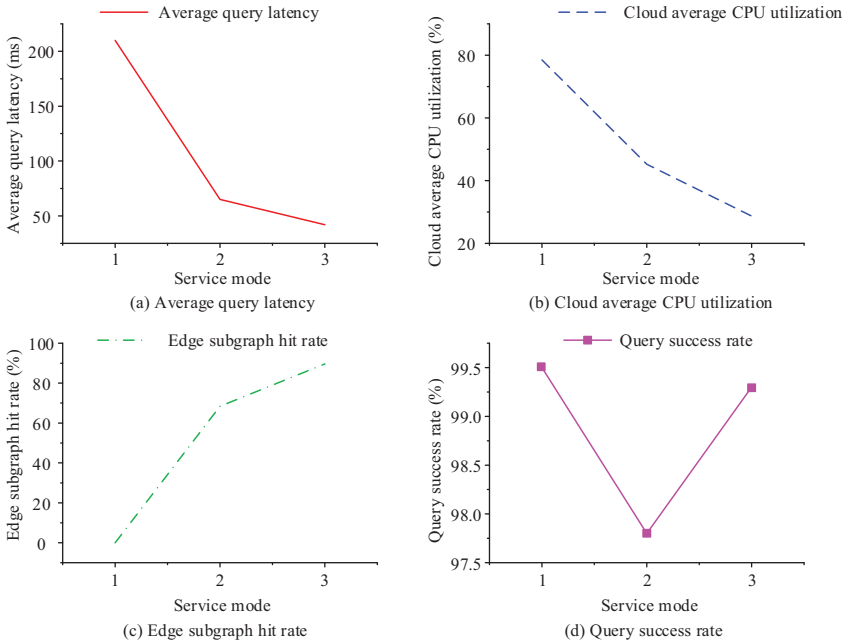


Figure 7 Performance evaluation of the edge-cloud collaborative service framework. Note: "1" represents pure cloud processing, "2" represents static edge caching, "3" represents proposed dynamic collaboration.

As shown in Figure 7, the proposed dynamic edge-cloud collaborative framework exhibited significant advantages in query latency, cloud load, and edge caching efficiency. Compared to pure cloud processing, its average query latency was significantly reduced to 42 ms, and cloud CPU utilization decreased from 78.5% to 28.7%. Compared to static edge caching, this framework maintained a similar query success rate of 99.3% while increasing the edge subgraph hit rate from 68.4% to 89.6%, achieving collaborative services with lower latency and higher resource utilization efficiency. Finally, to comprehensively evaluate the enhancement effect of the proposed method on business closed-loop capabilities, an in-depth test was conducted on a power distribution network fault diagnosis and isolation decision-making scenario. This scenario requires the system to quickly locate fault sections and generate isolation schemes based on multi-source data (protection action signals, fault waveforms, and equipment status).

The experiment compared the methods based on traditional rule engines, the methods based on single data source machine learning models, and

Table 3 Comparison of fault diagnosis and isolation performance

Evaluation Metric	Traditional Rule Engine	Single-Source Machine Learning	Graph-Driven Collaborative Optimization
Fault diagnosis accuracy (%)	85.6 ± 2.1	88.9 ± 1.7	95.3 ± 0.9
Average decision generation time (s)	8.2 ± 1.5	5.5 ± 0.8	3.8 ± 0.3
Scheme executability Verification pass rate (%)	82.4 ± 3.2	85.1 ± 2.5	94.7 ± 1.2
Comprehensive effectiveness index	72.1 ± 3.5	78.5 ± 2.8	92.6 ± 1.5

the graph-driven collaborative optimization method studied. The results are shown in Table 3.

It is worth noting that the mean $\pm$ standard deviation in Table 3 was calculated based on 10 independent repeated experiments. Each experiment randomly initialized the model parameters and divided the training and testing sets. The random seeds were set to 42, 123, 456, 789, 1024, 2048, 3021, 4096, 5123, and 6278, respectively. To verify whether the improvement of the proposed method compared to the comparative method was statistically significant, paired t-test was used for analysis, with a significance level set at $p < 0.05$.

The calculation formula for the comprehensive efficiency index was: $\mathrm{CEI} = 0.4 \times \mathrm{Accuracy}_{\mathrm{norm}} + 0.3 \times (1 - \mathrm{Time}_{\mathrm{norm}}) + 0.3 \times \mathrm{PassRate}_{\mathrm{norm}}$, where Accuracy, Time, and PassRate corresponded to the fault diagnosis accuracy, average decision generation time, and scheme feasibility verification pass rate in Table 2, respectively. Each sub item was mapped to the [0,100] interval using the minimum maximum normalization method, with the normalization criteria derived from the minimum and maximum values of the three comparison methods. The weight coefficients were determined using the Analytic Hierarchy Process, and were obtained by constructing a judgment matrix and calculating the consistency ratio $(\mathrm{CR} = 0.023 < 0.1)$, reflecting the evaluation principle of prioritizing accuracy, timeliness, and reliability.

As shown in Table 3, the graph-driven collaborative optimization method performed best across all metrics in the tested fault diagnosis and isolation scenarios. It achieved the highest fault diagnosis accuracy of 95.3% with minimal fluctuation. It also had the shortest average decision generation time, requiring only 3.8 seconds. Furthermore, its feasibility verification pass rate was leading at 94.7%. In terms of overall performance index, this method scored 92.6, higher than the traditional rule engine's 72.1 and the

single-source machine learning method's 78.5, demonstrating comprehensive advantages in accuracy, timeliness, and decision reliability. In addition, the paired t-test results indicated that the graph-driven collaborative optimization method had statistically significant improvements compared to traditional rule engines and single source machine learning methods. Among them, p-value for comparing the accuracy of fault diagnosis was 0.003, p-value for comparing the average decision generation time was 0.001, p-value for comparing the pass rate of scheme feasibility verification was 0.005, and p-value for comparing the comprehensive efficiency index was 0.002. The p-values for all comparison items were less than 0.01.

3.2 Application Verification in Typical Business Scenarios

To verify the dynamic performance and closed-loop optimization capability of the proposed method in actual power operations, three typical scenarios were selected for field testing: distribution situation awareness and risk warning, intelligent verification of relay protection settings, and source-grid-load-storage collaborative optimization scheduling. A comparative method was used, comparing the proposed graph-driven collaborative optimization method with two baseline methods: one based on a traditional business system using fixed rules and threshold discrimination; the other based on a data-driven optimization method using deep reinforcement learning. The experiments were conducted on a power grid simulation platform, continuously collecting time-series data at different time points or operational stages to evaluate the dynamic performance and enhancement effects of each method in actual business flows. First, in the distribution situation awareness and risk warning scenario: the experiment simulated five consecutive days of distribution network operation, recording the risk warning accuracy and warning lead time every four hours. Traditional methods are based on SCADA threshold alarms and simple logical rules, the data-driven method uses an LSTM network for time-series warnings, and the graph method integrates multi-source information and causal reasoning for warnings. The risk warning accuracy results are shown in Figure 8.

As shown in Figure 8, in continuous testing of power distribution risk warning scenarios, the graph-driven method consistently outperformed both the traditional rule-based method and the data-driven method in terms of risk warning accuracy. Looking at the time-series data, the accuracy of the graph-driven method steadily increased from an initial 88.5% to 96.7%, remaining above 90% with minimal fluctuations. The accuracy of the data-driven method gradually increased from 84.5% to 91.2%, while the accuracy

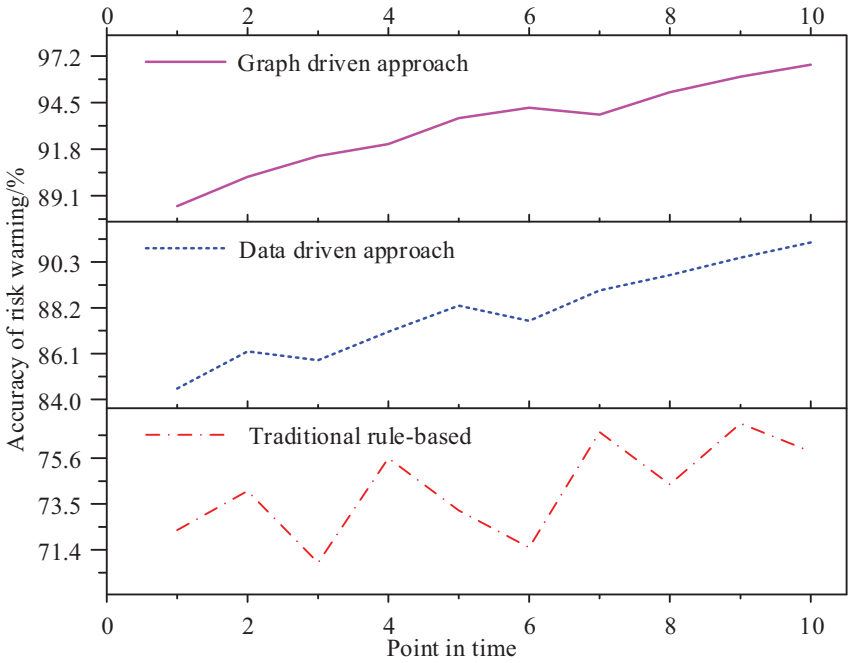


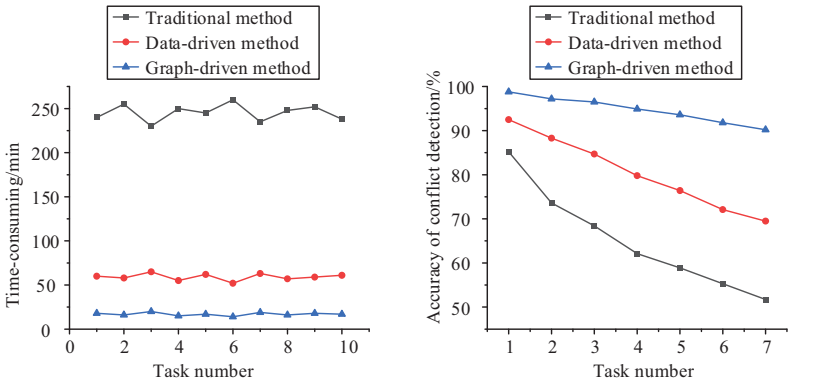
Figure 8 Comparison of risk warning accuracy over time.

Table 4 Comparison of changes in average early warning lead time (min)

Time Point (day-hour)	Traditional Rule-Based Method	Data-Driven Method	Graph-Driven Method
1-04	22	35	48
1-12	24	38	52
1-20	20	36	55
2-08	26	40	58
2-16	23	42	61
3-00	21	41	63
3-12	27	44	65
4-04	25	46	67
4-20	28	48	69
5-08	26	50	72

of the traditional rule-based method mainly fluctuated between 71% and 77%. The changes in the average warning lead time are shown in Table 4.

As shown in Table 4, in the five-day test of early warning time, the map-driven method consistently outperformed other methods, with its early



(a) Comparison of time consumption for fixed value verification tasks

(b) Comparison of accuracy in detecting conflicts in cross regional protection cooperation

Figure 9 Performance in the scenario of intelligent verification of relay protection settings.

warning time continuously increasing from 48 minutes to 72 minutes. The data-driven method's early warning time gradually improved from 35 minutes to 50 minutes, showing a moderate performance. The traditional rule-based method's early warning time fluctuated between 20 and 28 minutes, showing limited improvement and the lowest overall performance. These results demonstrated that the map-driven method had a significant and consistent advantage in the timeliness of risk early warning.

In the scenario of intelligent verification of relay protection settings, the experiment simulated 20 setting verification tasks submitted at different times within 24 hours, and recorded the verification time of each task. The traditional method used manual verification combined with offline calculation tools, the data-driven method used a machine learning model based on historical verification records for automatic verification, and the graph method used the online intelligent verification system proposed in the research. The results are shown in Figure 9.

Figure 9(a) shows that the graph-driven method had a significant advantage in terms of verification time, with the time for 20 tasks concentrated between 14 and 20 minutes, averaging about 17 minutes. The data-driven method took between 52 and 65 minutes, averaging about 59 minutes. The traditional method took as long as 230 to 260 minutes, averaging about 245 minutes. Figure 9(b) shows that as the complexity of the test scenario increased, the collision detection accuracy of all three methods showed a downward trend, but the graph-driven method consistently maintained above 90%, reaching 90.2% even in complex scenarios. The data-driven method

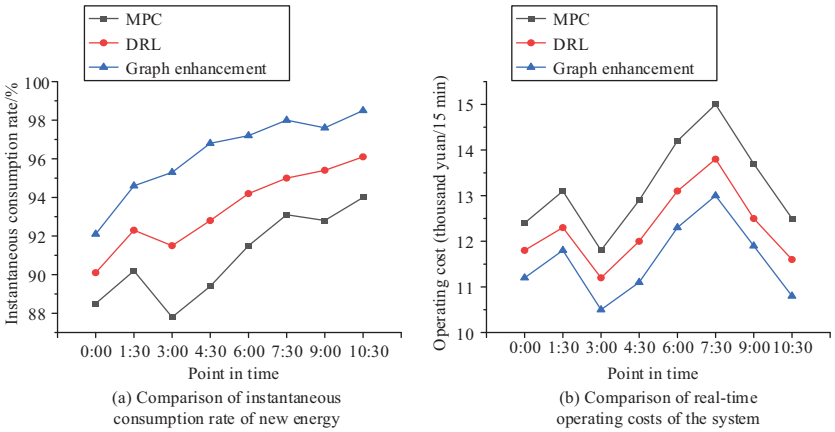


Figure 10 Continuous optimization effect in the source-grid-load-storage collaborative optimization scheduling scenario.

dropped from 92.5% to 69.5%, while the traditional method dropped significantly from 85.2% to 51.7%, highlighting the advantage of the graph-driven method in highly complex scenarios.

Finally, in the scenario of coordinated optimization scheduling of power generation, grid, load, and storage, the experiment recorded the renewable energy absorption rate and operating cost of the three methods within a continuous 8-hour scheduling cycle at 15-minute intervals. Among them, the traditional method adopted centralized model predictive control (MPC), the data-driven method used a deep reinforcement learning agent for real-time scheduling, and the graph method introduced auxiliary decision-making factors provided by knowledge graphs on the basis of traditional MPC. The results are shown in Figure 10.

Figure 10(a) shows that the graph-enhanced method consistently achieved the highest instantaneous renewable energy absorption rate across eight consecutive time points, steadily increasing from 92.1% to 98.5%. The data-driven method ranked second, rising from 90.1% to 96.1%, while the traditional MPC method had the lowest rate, fluctuating between 87.8% and 94.0%. Figure 10(b) indicates that the graph-enhanced method maintained the lowest real-time operating cost at all time points, decreasing from RMB 11.2k to 10.8k per 15 minutes (RMB [CNY] denotes Renminbi, with currency units expressed in thousands). The data-driven method was intermediate, ranging from RMB 11.6k to 13.8k, while the traditional MPC method had the highest cost, peaking at RMB 15.0k per 15 minutes. The graph method

Table 5 Comparison of risk warning accuracy under modality missing and delay (%)

Test Scenario	Missing/Delayed Modality	Complete Method	Data-Driven Method
Modality Missing	Fault recorder data	91.2	72.6
	Status text report	92.8	78.4
	Meteorological data	93.5	83.1
Modality delay	Fault recorder delay 30 s	90.5	70.3
	Fault recorder delay 60 s	87.9	62.7
	Fault recorder delay 90 s	84.6	55.8

demonstrated a sustained and significant dual advantage in both improving renewable energy absorption and reducing system operating costs.

3.3 Adaptive Verification under Multimodal Data Loss and Delay

To verify the adaptability of the method to incomplete or delayed arrival of multimodal data in real working conditions, two sets of comparative experiments were designed in the scenario of power distribution situational awareness: modal missing experiment and modal delay experiment. The modal loss experiment shielded three modalities: fault recording data, equipment status text reports, and meteorological data, to test the changes in the accuracy of risk warning. Modal delay experiment simulated the arrival of the three modes with delays of 30 s, 60 s, and 90 s, respectively, and tested the variation of warning accuracy with delay time. The experiment compared the proposed complete method with the data-driven method without introducing a knowledge graph, and the results are shown in Table 5.

From Table 5, when a single mode was missing, the early warning accuracy of the complete method remained above 91%, while the data-driven method dropped to 72.6% when fault recording was missing, which indicated that the knowledge map could effectively compensate the information of missing modes through semantic association and causal reasoning among multimodes. In the modal delay scenario, the complete method maintained an accuracy of 84.6% even after a 90 second delay, while the data-driven method reduced it to 55.8%, verifying the robustness advantage of knowledge graphs against temporal degradation.

4 Discussion

Compared with recent studies in the same field, this method has differentiated advantages in three aspects: multi-modal knowledge modeling, semantic

parsing depth, and service architecture. Wu et al. constructed a multi-modal knowledge graph for industrial equipment and achieved small-sample fault diagnosis through visual feature mapping [22]. However, their graph was mainly based on static fact associations without modeling spatiotemporal evolution or causal chains, making it difficult to support fault backtracking and situation inference in power systems. This study explicitly defined spatiotemporal attributes and causal edges at the schema layer, increasing the distribution risk warning lead time from 48 to 72 minutes, verifying the benefit of dynamic modeling for predictive tasks. Xie et al. achieved automatic knowledge graph construction from power plant maintenance reports, with entity recognition performance surpassing LSTM-CRF [23]. However, their work stopped at graph construction without involving semantic parsing or business integration, making it difficult to directly serve online decision-making. This study connected graph construction, semantic parsing, and edge-cloud collaboration into a complete closed loop. The proposed graph attention and feedback verification method outperformed baselines in intent recognition and query graph generation, achieving end-to-end mapping from natural language queries to executable decisions. Furthermore, the aforementioned studies all adopted a centralized architecture, which was difficult to adapt to wide-area distributed scenarios. The edge-cloud collaborative framework proposed in this study improved the edge subgraph hit rate from 68.4% to 89.6% and reduced cloud load by 62.8% through knowledge distribution and bidirectional correction, demonstrating engineering advantages in time-sensitive scenarios such as relay protection verification and source-grid-load-storage scheduling.

Further analysis revealed that the graph attention mechanism outperformed BiLSTM-CRF and GCN because it dynamically captured non-local semantic dependencies between query words and graph pattern elements, whereas sequence models were limited by local windows and static graph convolutions by fixed adjacency structures. The feedback verification mechanism suppressed the cumulative propagation of parsing errors through a generation-verification-correction closed loop, explaining why the full version outperformed the one without feedback. At the edge-cloud collaboration level, the dynamic knowledge distribution strategy achieved adaptive caching of hotspot knowledge by quantifying query access frequency and subgraph reachability distance, raising the edge subgraph hit rate from 68.4% to 89.6%. Graph anomaly detection in the bidirectional correction mechanism used GCN to score neighborhood consistency of entity embeddings, identifying implicit semantic conflicts beyond rule-based validation and supporting

continuous knowledge graph evolution. At the business scenario level, the increasing lead time of distribution risk warnings reflected the learning effect of causal reasoning capabilities – the richer the predecessor-successor causal edges extracted from historical event sequences, the greater the lead time for future risk chain deduction. The dual advantages in renewable energy consumption rate and operating cost for source-grid-load-storage scheduling stemmed from the knowledge graph's joint modeling of equipment response characteristics, meteorological correlation rules, and regulatory constraints. This enabled optimization algorithms to search for global optima within a more complete feasible domain, avoiding the out-of-distribution generalization failures that may plague purely data-driven deep reinforcement learning methods.

However, current graph construction still relies on expert annotation and rule templates, resulting in limited accuracy in extracting unstructured data. Furthermore, the adaptive capabilities of edge-cloud collaborative frameworks in extreme communication scenarios have not been fully validated. The adaptability of the proposed method was verified through experiments in Section 3.3 to address the issue of modal loss and delay that may occur in the practical operation of multimodal data. Its internal mechanism was that the knowledge atlas explicitly modeled the spatio-temporal correlation and causal dependency between different modal data. When a certain mode was missing, the graph structure reasoning ability of the atlas could indirectly infer the missing information from other modes through the correlation path; During modal delay, the predecessor-successor causal edges extracted from historical sequences could support state prediction based on incomplete observations, thereby mitigating the impact of temporal degradation on decision accuracy. This feature was difficult to implement in a single data source or rule-based approach, which constituted the unique advantage of graph-driven methods in multi-source heterogeneous environments. Future research could introduce large-model, few-shot learning to improve multi-modal end-to-end extraction capabilities and explore decentralized graph synchronization mechanisms to enhance system resilience and decision reliability in weak network environments.

5 Conclusion

To address the challenges of multi-modal data fusion and collaborative decision-making in novel power systems, a graph-driven intelligent fusion and collaborative optimization method was proposed. This method integrated

multi-modal knowledge graph construction, graph attention semantic parsing, and edge-cloud collaborative correction mechanisms, forming a closed-loop enhancement path from heterogeneous data to executable decisions. Experiments showed that the proposed method exhibited excellent performance in semantic parsing accuracy, query robustness, and multi-scenario transferability. Furthermore, it demonstrated good engineering practicality and decision enhancement capabilities in typical applications such as distribution situation awareness, relay protection verification, and source-grid-load-storage coordination.

Funding

This work was supported by the Science and Technology Fund Project of Guangxi Power Grid Corporation under Grant No. 046100KC24040010.

References

[1] Sy M F, Roman B, Kerrien S, Mendez D, Wajerowicz W, et al. Blue Brain Nexus: An open, secure, scalable system for knowledge graph management and data-driven science. Semantic Web, 2023, 14(4): 697–727. DOI: 10.3233/sw-222974.

[2] Meng S, Zhou J, Chen X, Liu Y, Lu F, Huang X. Structure-information-based reasoning over the knowledge graph: A survey of methods and applications. ACM Transactions on Knowledge Discovery from Data, 2024, 18(8): 1–42. DOI: 10.1145/3671148.

[3] Liu H, Zhang Z, Jia H, Zhang S, Yan L, Zhao Z. Construction and application of a knowledge graph for the spatial arrangement of underground powerhouses. Journal of Intelligent Construction, 2024, 2(3): 1–20. DOI: 10.26599/Jic.2024.9180026.

[4] Yang Y, Yang M, Shangguan S, Cao Y, Jiang P. A novel method to build knowledge graph models for the configuration and operation design of smart and connected industrial products. Journal of Computational Design and Engineering, 2024, 11(2): 327–344. DOI: 10.1093/jcde/qwae033.

[5] Sun F, Zhang X, Wei Z, Wang J, Feng Z, Lu J. A hybrid framework of symbolic and embedding-based logic for temporal knowledge graph reasoning. IEEE Internet of Things Journal, 2025, 13(2): 2085–2098. DOI: 10.1109/JIOT.2025.3630489.

[6] Xu T, Zou Z, Hu R, Zhou L, Yao Z, Zhang W. A construction method of dispatching operation knowledge graph of hydro power stations based on BiGRU+CRF deep learning model. Journal of Electric Power Science and Technology, 2025, 40(1): 180–189. DOI: 10.19781/j.issn.1673-9140.2025.01.019.

[7] Mandal B, Roy P K. Dynamic economic dispatch problem in hybrid wind based power systems using quasi oppositional based chaotic honey badger algorithm. Electric Power Components and Systems, 2024, 52(9): 1543–1568. DOI: 10.1080/15325008.2023.2240800.

[8] Zhang M, Zhen Z, Liu N, Zhao H, Sun Y, Feng C. Optimal graph structure based short-term solar PV power forecasting method considering surrounding spatio-temporal correlations. IEEE Transactions on Industry Applications, 2022, 59(1): 345–357. DOI: 10.1109/TIA.2022.3213008.

[9] Einfalt A, Aryan P R, Sabou M, Fernbach A, Frischenschlager A. Realisation of grid-friendly charging considering usability by knowledge graph enabled explainability. IET Conference Proceedings CP798. Stevenage, UK: The Institution of Engineering and Technology, 2022, 2022(3): 596–600. DOI: 10.1049/icp.2022.0778.

[10] Wang Z, Li L, Zeng D D. Symbolic knowledge reasoning on hyper-relational knowledge graphs. IEEE Transactions on Big Data, 2024, 11(2): 578–590. DOI: 10.1109/TBDATA.2024.3423670.

[11] Zou Z, Wang B, Chen T. Research on power data security full-link monitoring technology based on alternative evolutionary graph neural architecture search and multi-modal data fusion. Discover Applied Sciences, 2025, 7(6): 633. DOI: 10.1007/s42452-025-07247-z.

[12] Vahidi S, Ghafouri M, Au M, Kassouf M, Mohammadi A, Debbabi M. Security of wide-area monitoring, protection, and control (WAMPAC) systems of the smart grid: A survey on challenges and opportunities. IEEE Communications Surveys & Tutorials, 2023, 25(2): 1294–1335. DOI: 10.1109/COMST.2023.3251899.

[13] Srivastava A, Liu C C, Stefanov A, Basumallik S, Hussain M M, Somda B. Digital twins serving cybersecurity: More than a model: Cybersecurity as a future benefit of digital twins 2. IEEE Power and Energy Magazine, 2024, 22(1): 61–71. DOI: 10.1109/MPE.2023.3325196.

[14] Mendoza M A T, Segundo-RamÃrez J, Gurrola A E, Visairo-Cruz N, Guitierrez C A N, Torres U. Digital twin adaptive remedial action scheme for preventing voltage collapse. IEEE Journal of Emerging and

Selected Topics in Industrial Electronics, 2024, 6(2): 523–535. DOI: 10.1109/JESTIE.2024.3465429.

[15] Pingyan M, Kai L, Yanqian L, You W, Tao L. Research on the standardization of AI-driven data security communication protocols for power trading networks. Journal of ICT Standardization, 2025, 13(3): 257–280. DOI: 10.13052/jicts2245-800X.1332.

[16] Jie Q, Weicong T, Ren L, Lichen X, Zhiding Z. Research on the architecture and i mplementation of power archive information platform based on international and local stan dards. Journal of ICT Standardization, 2026, 14(2): 259–294. DOI: 10.13052/jicts2245-800X.1426.

[17] Shittu M A, Shittu H A, Adeleke O J, Adeleke O J. Digital twin modeling for real time monitoring and fault detection in smart substations. International Journal of Industrial Engineering, 2023, 14(2): 25–44. DOI: 10.34218/IJIERD_14_02_003.

[18] Li K, Wang Y, Zhu T, Li J, Ren J. Knowledge graph-based multi-modal neural networks for smart-grid defect detection. Engineering Reports, 2024, 6(9): e12824. DOI: 10.1002/eng2.12824.

[19] Shi J, Zhang W, Bao Y, Gao D W, Wang Z. Load forecasting of electric vehicle charging stations: Attention based spatiotemporal multi-graph convolutional networks. IEEE Transactions on Smart Grid, 2023, 15(3): 3016–3027. DOI: 10.1109/TSG.2023.3321116.

[20] Chen C, Wang Y, Cui M, Zhao J, Bi W, Chen Y. Data-driven detection of stealthy false data injection attack against power system state estimation. IEEE Transactions on Industrial Informatics, 2022, 18(12): 8467–8476. DOI: 10.1109/TII.2022.3149106.

[21] Li B, Yang L L, Maunder R G, Sun S, Xiao P. Heterogeneous graph neural network for power allocation in multicarrier-division duplex cell-free massive MIMO systems. IEEE Transactions on Wireless Communications, 2023, 23(2): 962–977. DOI: 10.1109/TWC.2023.3284263.

[22] Wu Y, Liu F, Wan L, Wang Z. Intelligent fault diagnostic model for industrial equipment based on multi-modal knowledge graph. IEEE Sensors Journal, 2023, 23(21): 26269–26278. DOI: 10.1109/JSEN.2023.3316473.

[23] Xie T, Tao S, Li Q, Wang H, Jin Y. A lattice LSTM-based framework for knowledge graph construction from power plants maintenance reports. Service Oriented Computing and Applications, 2022, 16(3): 167–177. DOI: 10.1007/s11761-022-00338-4.

Biographies



Qi Chen, female, was born in January 1998 and is a native of Guangxi, China. She holds a Master's degree and currently works as a Specialist at Guangxi Power Grid Co. Ltd. Her main research direction focuses on Artificial Intelligence, and she is engaged in related work in the field of power grid intelligence.



Wei Wang, male, was born in September 1993 and is a native of Guangxi, China. He holds a bachelor's degree and works as an Engineer, with his professional focus on Electrical Engineering and Technology Management, engaging in related technical and management work in the power industry.



Yun Dong, female, was born in November 1989. She holds a Master's degree and serves as a Senior Engineer, with her professional focus on Power Artificial Intelligence, devoting herself to the research and application of artificial intelligence technology in the power field.



Chunfang Yi, female, was born in September 1979. She holds a bachelor's degree and serves as a Senior Engineer, with her professional focus on Electrical Engineering and Automation, engaging in technical research and practical application of related technologies in the power industry.